

# A Monte Carlo study for the shielding of $\gamma$ backgrounds induced by radionuclides for CDEX<sup>\*</sup>

LI Lei(李磊)<sup>1,2</sup> YUE Qian(岳骞)<sup>2;1)</sup> TANG Chang-Jian(唐昌建)<sup>1</sup> CHENG Jian-Ping(程建平)<sup>2</sup>  
 KANG Ke-Jun(康克军)<sup>2</sup> LI Jian-Min(李荐民)<sup>2</sup> LI Jin(李金)<sup>2</sup> LI Yu-Lan(李玉兰)<sup>2</sup>  
 LI Yuan-Jing(李元景)<sup>2</sup> MA Hao(马豪)<sup>2</sup> H. T. Wong(王子敬)<sup>3</sup>  
 XUE Tao(薛涛)<sup>2</sup> ZENG Zhi(曾志)<sup>2</sup>

(on behalf of the CDEX/TEXONO collaboration)

<sup>1</sup> Department of Applied Physics, Sichuan University, Sichuan 610064, China

<sup>2</sup> Department of Engineering Physics, Tsinghua University, Beijing 100084, China

<sup>3</sup> Institute of Physics, Academia Sinica, Taipei 11529, China

**Abstract:** The CDEX (China Dark matter EXperiment) Collaboration will carry out a direct search for WIMPs (Weakly Interacting Massive Particles) using an Ultra-Low Energy Threshold High Purity Germanium (ULE-HPGe) detector at the CJPL (China JinPing deep underground Laboratory). A complex shielding system was designed to reduce backgrounds and a detailed GEANT4 Monte Carlo simulation was performed to study the achievable reduction of  $\gamma$  rays induced by radionuclides and neutron backgrounds by  $D(\gamma,n)p$  reaction. Furthermore, the upper level of allowed radiopurity of shielding materials was estimated under the constraint of the expected goal. Compared with the radiopurity reported by other low-background rare-event experiments, it indicates that the shielding used in the CDEX can be made out of materials with obtainable radiopurity.

**Key words:** Monte Carlo, simulation, dark matter, underground experiment, radionuclides

**PACS:** 24.10.Lx, 25.20.-x      **DOI:** 10.1088/1674-1137/35/3/013

## 1 Introduction

The CDEX collaboration will carry out a direct search for WIMPs using a ULE-HPGe detector [1–3]. WIMPs are known as strong candidates for cold dark matter. The experiment site, the CJPL, is located in one of several tunnel cavities in Jinping Mountain in the Sichuan Province, China. The minimum depth is about 2500 m rock overburden, and the main component of the rocks around the CJPL is marble with low radioactivity. Therefore, the CJPL provides good natural conditions for dark matter search and other low-background experiments.

For this low-energy low-background and rare-event experiment, the first challenge is to suppress the backgrounds to a great extent, and the CDEX collaboration has designed a complex shielding system to achieve that. The backgrounds of deep under-

ground experiments are mainly caused by (i) cosmic rays, (ii) environmental radiations and (iii) the intrinsic radiation of the detectors. Dominant environmental radiations are due to  $\gamma$  rays and concomitant neutrons induced by radionuclides. This paper studies the achievable reduction from a shielding system against  $\gamma$  radiation originating from the shielding materials and the rock of the laboratory with GEANT4 [4], which is a general purpose Monte Carlo code.

For the CDEX, a environmental background index of less than 0.1 cpd/(keV·kg) (cpd: counts per day) in the ULE-HPGe detector at the 100 keV range is expected. Based on that goal, the proposal of the shielding system and a hypothetical HPGe detector array (fiducial mass 1 ton), this paper estimates the upper level of allowed radiopurity of different shielding materials. Moreover, this work takes notice of the shielding of the neutron backgrounds induced by a  $D(\gamma,n)p$  reaction.

Received 21 June 2010, Revised 5 November 2010

\* Supported by National Natural Science Foundation of China (10935005,10945002)

1) E-mail: yueq@mail.tsinghua.edu.cn

©2011 Chinese Physical Society and the Institute of High Energy Physics of the Chinese Academy of Sciences and the Institute of Modern Physics of the Chinese Academy of Sciences and IOP Publishing Ltd

## 2 Shielding system and simulation geometry

The design proposal of the shielding system in the CDEX is shown schematically in Fig. 1. The outermost layer is 1 m PE(polyethylene) for decelerating and absorbing fast neutrons. Then, a 20 cm lead is situated for reducing the environmental  $\gamma$  ray backgrounds. The next layer is a 15 cm steel support structure. Then, there is a 20 cm PE(B) (Boron-doped-polyethylene) layer to absorb of thermal neutrons. The innermost layer is 10 cm OFHC(oxygen-free highly-conductive copper) for absorbing residual  $\gamma$  rays. The space inside the copper layer, with a dimension of  $2(W) \text{ m} \times 2.5(D) \text{ m} \times 2(H) \text{ m}$ , is for the ULE-HPGe detector and is large enough to accommodate a ton-scale mass HPGe detector array. To reduce the background of radon gas, the inner space of shielding will be refreshed continuously by highly pure nitrogen gas.

During the simulation, we tried to use as much actual geometry as possible. However, there were two main approximations. Firstly, based on the simulation results, for normal incident  $\gamma$  with 4 MeV mono-energy(the upper  $\gamma$  energy in this work), we know that the flux was reduced to less than 10% after passing through a 50 cm sur-

rounding rock was considered. Secondly, the 15 cm support structure layer was substituted by air in the primary study because we were not sure whether it had a geometric structure(most likely it is of a steel frame structure). The parameters used for constructing the geometry in simulation, are listed in Table 1.

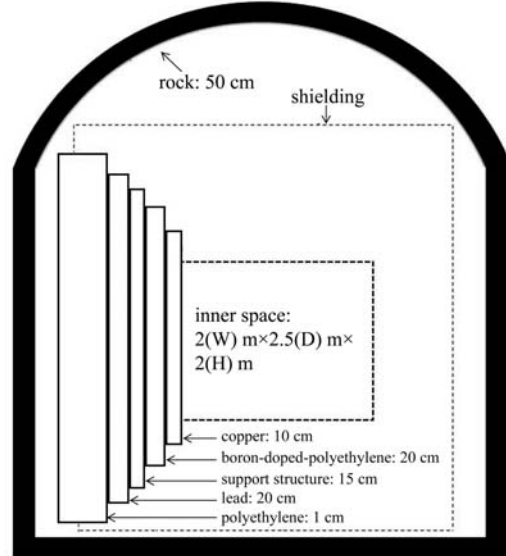


Fig. 1. Schematic diagram for the proposal of the shielding system and surrounding rock. The coverage of actual shielding is  $4\pi$ , and only the section is shown.

Table 1. Parameters in simulations.

	thickness/cm	outside size/cm			density/(g/cm <sup>3</sup> )
		width	depth	height	
rock(tunnel)	50	750	4000	850	2.7
PE	100	650	1000	560	0.96
lead	20	330	380	330	11.35
support	15	290	340	290	0.13 (air)
PE(B)	20	260	310	260	0.99
copper	10	220	270	220	8.96
inner space	–	200	250	200	–

## 3 Radionuclides and the Monte Carlo simulation process

### 3.1 Radioactive nuclide

The dominant  $\gamma$  ray backgrounds are due to  $^{40}\text{K}$ ,  $^{232}\text{Th}$  and  $^{238}\text{U}$  and their daughter. In the primary study, we focused on the  $\gamma$  rays induced by those radionuclides. They are primordially occurring and exist in all materials, and in this work, three  $\gamma$  sources were considered, including the surrounding rock, the

lead and the copper layer.

The rock samples at the CJPL were analyzed to determine its radiopurity and the results are shown in Table 2. In Table 3, the reported radiopurity of the shielding materials by other low-background experiments are listed [5–7].

Table 2.  $^{232}\text{Th}$ ,  $^{238}\text{U}$  and  $^{40}\text{K}$  of rock at CJPL.

	nuclide		
	$^{232}\text{Th}$	$^{238}\text{U}$	$^{40}\text{K}$
rock (<66.3) ppb	(147.3±16.4) ppb	(<36.4) ppm	

Table 3. Reported radiopurity of shielding materials.

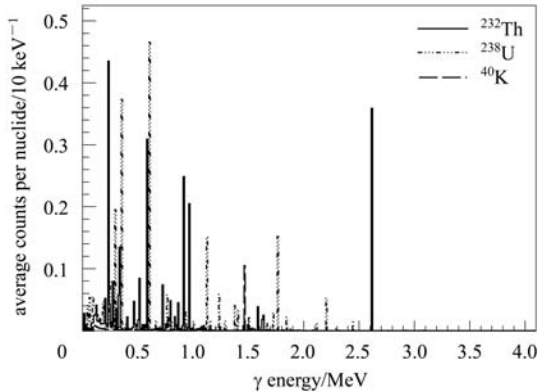
Exp.	material	nuclide		
		$^{232}\text{Th}/$ ppb	$^{238}\text{U}/$ ppb	$^{40}\text{K}/$ ppm
KIMS*	lead (ancient)	<0.03–0.2	<0.02–0.7	<0.3
LNGS*	lead (modern)	<4.91	<2.46	<9.93
XENON 100*	lead (outer)	<0.18	<0.08	0.47±0.1
	lead (inner)	<0.14	<0.06	<0.05
	copper	<0.007	<0.006	<0.002

\*Unit conversion.

### 3.2 Description of the Monte Carlo simulation process

#### 3.2.1 Simulation process

The simulation process was divided into two steps. Firstly, the  $\gamma$  energy spectrum by decay of each radionuclide in different material (rock, lead and copper) was obtained with particle decay processes installed in GEANT4. In the  $\sim 100$  keV range, the  $\gamma$  energy spectrum is slightly different for different materials, which is mainly due to the bremsstrahlung of the electron. Fig. 2 shows the  $\gamma$  energy spectrum in the lead material. Assuming secular equilibrium, we obtained the average  $\gamma$  number ( $\eta$ ) induced per nuclide for the next calculation, shown in Table 4.

Fig. 2. The  $\gamma$  energy spectrum of radionuclides in lead material.

Secondly, the initial conditions of the next simulations were designed as the following: 1) Construct the simulation geometry as described in Section 2. 2) Consider three kinds of  $\gamma$  ray sources, including the rock, lead and copper layer. 3) Initial  $\gamma$  energy was randomly sampled from the energy spectrum, obtained in the first step. 4) Set the direction of the initial isotropic momentum. For  $\gamma$  transportation with GEANT4, the physical processes treated in

our work were based on a low energy model including Rayleigh scattering, photoelectric effect, Compton scattering and the pair-production process. In addition, the photonuclear process was considered to study the neutron backgrounds induced by  $D(\gamma, n)p$  reaction. Firstly, we consider the contribution to the background from the surrounding rock and shielding materials, and then estimate the upper level of allowed radiopurity of materials. Lastly, we discuss the neutron induced by  $D(\gamma, n)p$ .

Table 4. The average  $\gamma$  number  $\eta$  induced per nuclide in different materials.  $\gamma_e$  is the relative error.

material	nuclide					
	$^{232}\text{Th}$		$^{238}\text{U}$		$^{40}\text{K}$	
	$\eta$	$\gamma_e(\%)$	$\eta$	$\gamma_e(\%)$	$\eta$	$\gamma_e(\%)$
rock	2.86	0.17	2.43	0.15	0.153	0.8
lead	2.97	0.16	2.64	0.14	0.195	0.7
copper	2.91	0.16	2.53	0.15	0.173	0.7
Ref.*	2.50	–	2.17	–	0.116	–

\*[8] only considered the  $\gamma$  induced by decay process. Our simulation included not only the  $\gamma$  from decay process, but also the concomitant  $\gamma$  additionally, which is mainly due to the bremsstrahlung of electron. One can see the difference between the Ref. [8] and our simulation results. If we did not include the concomitant  $\gamma$  in the simulation, our results match the data of Ref. [8] within one standard deviation.

#### 3.2.2 Variance reduction

The relative error ( $\gamma_e$ ) represents the statistical precision as a fractional result with respect to the estimated mean ( $\bar{p}$ ) and is defined as

$$\gamma_e = \frac{\sigma}{\sqrt{N\bar{p}}}. \quad (1)$$

Here,  $\sigma$  denotes the standard deviation and  $N$  is the sample size. In this work, the relative error ( $\gamma_e$ ) was calculated corresponding to one standard deviation.

Since in such a low background experiment shielding is required to reduce the background to a great extent, our work is then a deep penetration problem. To reduce the computing time and relative errors, we applied two kinds of sophisticated techniques of variance reduction, including the importance sampling and cross-section biasing installed in GEANT4. During the simulations, we have compared the results of the variance reduction method with the analogue simulation results step by step and they met each other quite well.

## 4 Monte Carlo simulation results

### 4.1 Shielding effectiveness

The shielding system is shown in Fig. 1. For

evaluating the  $\gamma$  ray reduction achievable by this system, we designed two tallies in simulations. The first one is the  $\gamma$  flux attenuation by each shielding layer. The results are shown in Fig. 3 ( $\gamma_e < 3.2\%$ ). Fig. 3(a) presents the flux attenuation sequentially transmitted through the shielding layer. Fig. 3(b) shows the flux spectrum on the copper layer's inner surface. The results indicate that the  $\gamma$  rays induced by radionuclides could be effectively reduced by shielding.

For  $\gamma$  rays starting in the lead and copper layers with different positions, we want to know their contribution to the flux in the inner space (inside the copper layer). So the second tally is the penetration

probability through the copper layer's inner surface of  $\gamma$  rays. From inside to outside, the 20 cm lead layer was divided into 20 bins, and each 1 cm bin was a statistical interval. Similarly, the 10 cm copper was divided into 10 intervals. The results are shown in Fig. 4. Fig. 4(a) shows the  $\gamma$  rays starting in the lead layer ( $\gamma_e < 4.2\%$ ), and we fitted it with an exponential function. As shown in the figure, the penetration probability decreases exponentially with the increase of distance. In the case of copper, there are similar results, shown in Fig. 4(b) ( $\gamma_e < 1.6\%$ ). From Fig. 4, we can estimate the  $\gamma$  flux changes in the inner space with the thickness of lead and copper layer.

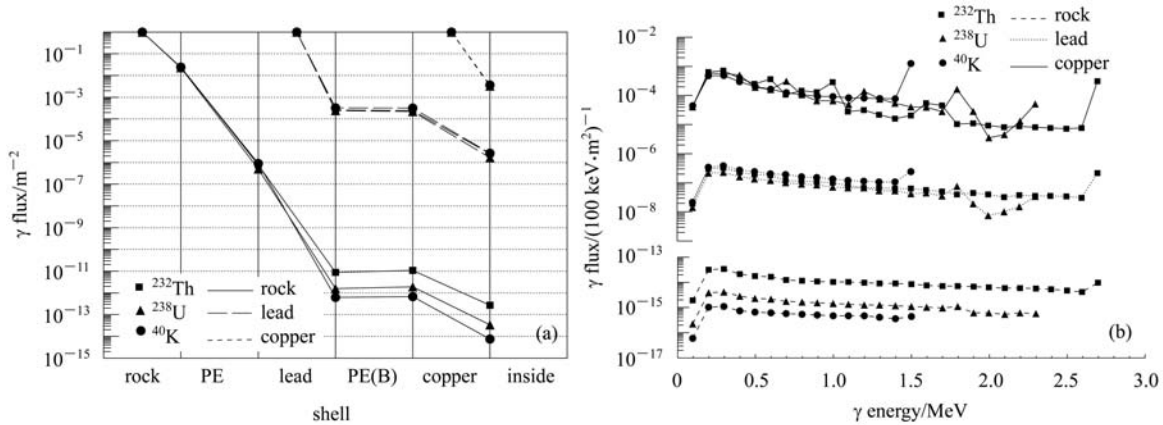


Fig. 3. (a) represents the flux attenuation per source  $\gamma$  transmitted through the shielding layer sequentially ( $\gamma_e < 3.2\%$ ); (b) is the flux spectrum per source  $\gamma$  on the copper layer's inner surface.

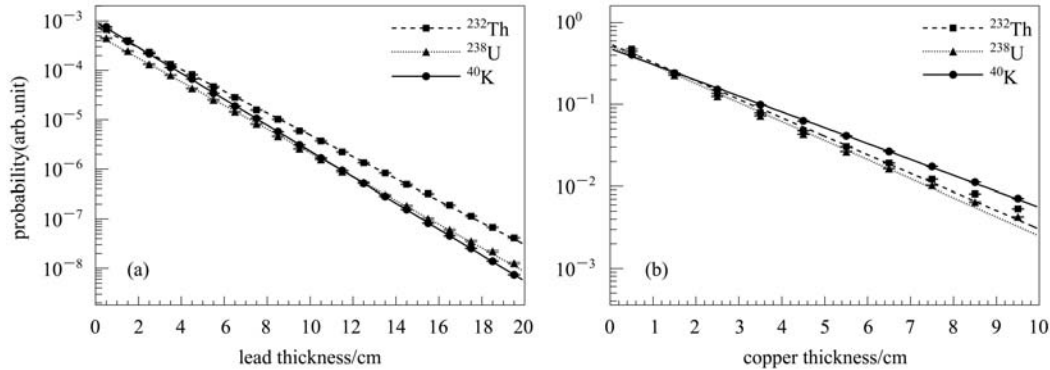


Fig. 4. The relationship between layer thickness and  $\gamma$  penetration probability through the copper layer's inner surface. All results are normalized to one source  $\gamma$ . (a) is for the  $\gamma$  rays starting in the lead layer ( $\gamma_e < 4.2\%$ ), and (b) for the copper layer ( $\gamma_e < 1.6\%$ ).

## 4.2 Estimates of radiopurity

For estimating the upper level of allowed radiopurity of shielding materials, a hypothetical HPGe detector array was constructed in simulations, as described in Fig. 5. A HPGe element is a cylinder ( $\phi 6.2 \text{ cm} \times 6.2 \text{ cm}$ , 1 kg), which will be used and treated as a single readout in future experiments. The

horizontal and vertical gaps are 1 cm and 2 cm respectively. The HPGe detector array consists of a  $10 \times 10 \times 10$  fiducial detector array (1 ton) and four layers as a surrounding active  $4\pi$ -veto.

For the CDEX, an environmental background index of less than 0.1 cpd/(keV.kg) in the ULE-HPGe detector at the 100 keV range is expected. In our

estimation, this goal was equivalent to 0.12 cps (cps: counts per second) with 1000 kg ULE-HPGe mass, 100 keV energy region and 86400 s per day. In the primary study, we do not just consider backgrounds in the range of 100 keV, but the whole energy region. This is due to not taking all assemblies into account and to conservative estimation.

The  $\gamma$  event meeting the following conditions was treated as background: 1), It was a single-hit (i.e. just deposit energy in one fiducial HPGe element). 2), It can not be vetoed. The event was treated as vetoed if its energy deposition in any one veto HPGe element was larger than the threshold, which was set at 10 keV for conservative estimation.

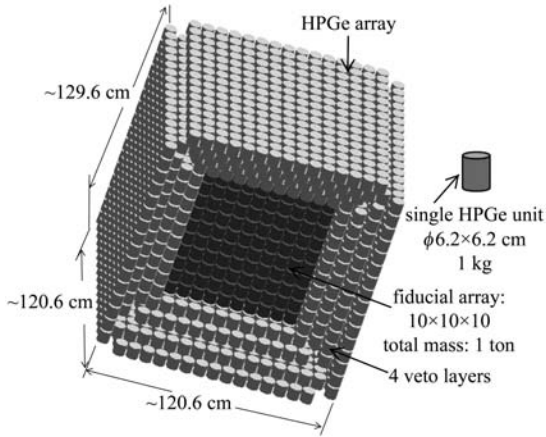


Fig. 5. Diagram of hypothetical the HPGe detector array.

The hypothetical HPGe detector array was placed in the center of shielding system in the simulations, and the tally was the counts of backgrounds ( $C_b$ ) discussed above. The results are listed in Table 5. The equation used for calculation was

$$\frac{R_A \cdot m}{A} \cdot (1 - e^{-\lambda t}) \cdot \eta \cdot C_b = C_g. \quad (2)$$

Here  $R_A$  (g/g) is the radionuclide activity,  $m$  is the mass of  $\gamma$  source material,  $A$  is atomic weight,  $\lambda$  is corresponding decay constant,  $t$  is time,  $\eta$  is the average  $\gamma$  number induced per nuclide,  $C_b$  is backgrounds produced per source  $\gamma$ , and  $C_g$  is background counts.

Table 5. The averaged background counts ( $C_b$ ) per source  $\gamma$  in the HPGe detector array.

nuclide		$\gamma$ source		
		rock	lead	copper
$^{232}\text{Th}$	$C_b$	$8.94 \times 10^{-16}$	$1.05 \times 10^{-8}$	$1.79 \times 10^{-5}$
	$\gamma_e(\%)$	5.5	3.3	1.8
$^{238}\text{U}$	$C_b$	$1.4 \times 10^{-16}$	$7.32 \times 10^{-9}$	$1.71 \times 10^{-5}$
	$\gamma_e(\%)$	4.4	4.1	1.9
$^{40}\text{K}$	$C_b$	$3.47 \times 10^{-17}$	$1.07 \times 10^{-8}$	$2.66 \times 10^{-5}$
	$\gamma_e(\%)$	8.3	3.3	1.5

Substituting the data (Table 2 ( $\eta$ ) and Table 5 ( $C_b$ )) into Eq. (2), we can obtain the total backgrounds ( $C_g$ ) induced by rock radioactivity is less than 0.01 cpd. So it was shielded very well, and can be negligible. On the other hand, with the data in Table 5 ( $C_b$ ) and Eq. (2), we could estimate the upper level of allowed radiopurity of lead and copper material under the constraint of the expected goal ( $C_g$ ). The results are listed in Table 6. Compared with the reported radiopurity in Table 3, it shows that the estimated radionuclide activity was consistent with the reported results on order of magnitude. Moreover, those results were all obtained under conservative conditions and several discrimination methods could be used in experiment to reduce backgrounds. The results discussed above, indicate that the shielding of the CDEX could be made out of materials with obtainable radiopurity.

Table 6. The estimated upper level of allowed radiopurity of lead and copper ( $R_A$ ).  $C_g$  is the expected backgrounds counts.

material	mass/ton	total $C_g$ /cps	nuclide					
			$^{232}\text{Th}$		$^{238}\text{U}$		$^{40}\text{K}$	
			$C_g$ /cps	$R_A$	$C_g$ /cps	$R_A$	$C_g$ /cps	$R_A$
lead	145	0.03	0.01	0.56 ppm	0.01	0.29 ppm	0.01	0.13 ppm
copper	27.5	0.03	0.01	1.77 ppb	0.01	0.68 ppb	0.01	0.27 ppb

### 4.3 D( $\gamma$ ,n)p induced neutron

The ratio of H(Hydrogen) and D(Deuterium) is about 1/7000 in nature and the excitation curve of D( $\gamma$ ,n)p ( $Q = -2.24$  MeV) is shown in Fig. 6(a) [9], which changes rapidly with  $\gamma$  energy. Because

of the large-scale use of hydrogen-rich materials such as polyethylene and Boron-doped-PE, the  $\gamma$  induced neutron may produce backgrounds.

The main contribution to the neutron backgrounds from the D( $\gamma$ ,n)p reaction is due to the 2.61 MeV  $\gamma$ -line of  $^{208}\text{Tl}$ , which is produced in the

decay chain of  $^{232}\text{Th}$ . As shown in Fig. 2, the other  $\gamma$  lines originating in the primordial U/Th decay chains with energies above 2.24 MeV (except 2.61 MeV) exhibit significantly lower intensities. Thus, all the calculations were done for the energy of this  $^{208}\text{Tl}$  line. In simulations, we designed a  $\gamma$  source with 2.61 MeV mono-energy and used cross-section biasing techniques for variance reduction.

The induced neutron energy spectrums are shown in Fig. 6(b), which indicate that the neutron kinetic energy is centered on  $\sim 200$  keV. The possibility of neutrons produced per source  $\gamma$  is listed in Table 7

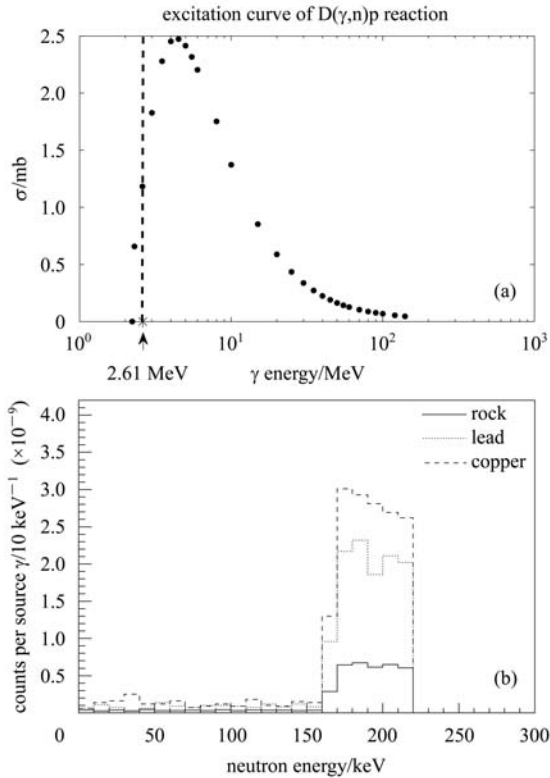


Fig. 6. (a) The excitation curve of  $D(\gamma,n)p$  reaction; (b) Neutron energy spectra for initial  $\gamma$  in rock, lead and copper material, respectively.

for all situations. If taking  $<66.3$  ppb,  $<4.91$  ppb and  $<0.007$  ppb  $^{232}\text{Th}$  concentration (data in Table 2 and Table 3 for rock, lead and copper, respectively) into account, we could get that the total neutron yield in the shielding materials is  $<13$  cpd. For lead and copper simulations, there were rare neutrons transmitted through the copper layer. So it will only produce rare backgrounds.

Table 7. The possibility ( $p$ ) of neutron produced per source  $\gamma$ .

$\gamma$ source	rock	lead	copper
$p$	$4 \times 10^{-9}$	$1.3 \times 10^{-8}$	$1.7 \times 10^{-8}$
$\gamma_e(\%)$	1.6	2.8	2.4

## 5 Summary and conclusion

The CDEX Collaboration will carry out a direct search for WIMPs using a ULE-HPGe detector, and a GEANT4 Monte Carlo study of the shielding system designed for the experiment was performed. The achievable reduction of  $\gamma$  rays induced by radionuclides was studied in detail, and with the simulation presented here, it indicates that those backgrounds could be reduced very effectively by shielding.

Furthermore, we studied the neutron induced by  $D(\gamma,n)p$  in shielding materials. Because it has a very low yield ( $<13$  cpd) and its kinetic energy is centered on  $\sim 200$  keV, it will only produce rare backgrounds.

With the hypothetical HPGe detector array, we calculated that the backgrounds induced by rock radioactivity is less than 0.01 cpd. In addition, under the constraint of expected goal, we estimated the upper level of allowed radiopurity of the shielding materials: 1), For lead,  $^{232}\text{Th}$ : 0.56 ppm,  $^{238}\text{U}$ : 0.29 ppm and  $^{40}\text{K}$ : 0.13 ppm. 2), For copper,  $^{232}\text{Th}$ : 1.77 ppb,  $^{238}\text{U}$ : 0.68 ppb and  $^{40}\text{K}$ : 0.27 ppb. Our study indicates that the shielding of the CDEX can be made out of materials with obtainable radiopurity.

## References

- KANG K J et al. Status and Prospects of a Deep Underground Laboratory in China. Journal of Physics: Conference Series. 2010. 012028. 1–3
- LI Xin et al. HEP & NP, 2007, **31**(6): 564–569 (in Chinese)
- YUE Qian et al. HEP & NP, 2004, **28**(8): 877–880 (in Chinese)
- GEANT4 web-page. <http://geant4.web.cern.ch/geant4/index.shtml>
- Danevich F A et al. Nucl. Instrum. Methods A, 2009, **603**: 328–332
- Arpesella C. Appl. Radiat. Isot, 1996, **47**: 991–996
- Alexander Kish. XENON100 Talks, 2010
- National Nuclear Data Center, NuDat 2.5. <http://www.nndc.bnl.gov/nudat2/>
- Evaluated Nuclear Data File, JENDL-3.3 Japan Atomic Energy Agency. <http://www.nndc.bnl.gov/sigma/getInterpreted.jsp?valid=9264&mf=3&mt=28>, 2002